

Table 1
Test rig dimensions.

Component dimension	Size
Gable thickness	41 mm
Gable height	350 mm
Gable width	540 mm
Flywheel diameter	275 mm
Flywheel width	117 mm
Drive shaft length	527 mm
Torque arm length	150 mm

for clutch engagement with a separate oil supply. One lubrication system and the hydraulic system pump oil into the clutch shaft channels through an oil divider mounted on the previously mentioned door. An oil filter for the lubrication oil is also mounted on the door as well as the solenoid servo valve which controls the engagement pressure.

The lubrication oil tank has a volume of 20 l. The oil is pumped by fixed displacement gear pumps through the two circulation systems, both of which has a maximum flow rate of 10 l/min. The primary circulation system pump the lubricant through the clutch axle into the friction interface, while a very small fraction of the oil is directed to lubricate the bearings of the drive shaft. In the secondary circulation system, oil is pumped through a filter and a heat exchanger where the oil temperature is controlled by means of water cooling. There is also a possibility to heat the oil in the tank using a suspension heater allowing for control of the test temperature with a variation less than 2 °C. The dimensions of the test rig is summarized in Table 1.

2.2. Sensors

A number of different sensors are installed in the rig to measure the clutch characteristics. The sensor working ranges and their resolution is summarized in Table 2.

The vertical torque arm is in direct contact with a load sensor. The sensor is mounted in a holder attached to the bottom plate. The load cell output voltage is converted to load in the control software. The temperature is measured in the separator discs by the use of thermocouples (type K). These thermocouples are metal sheathed with a diameter of 0.5 mm with a specified response time of 14 ms. The short response time allows for the capture of the fast changes in temperature during clutch engagement. One thermocouple is also used to monitor the oil tank temperature.

One thermocouple is installed in each separator disc. The thermocouples are inserted into holes of diameter 0.8 mm drilled from the separator disc edges. Three different materials were tested in the interface between the thermocouple and the hole wall in terms of temperature response performance. Material one is simply the ATF which will fill the gap between thermocouple and disc wall during test rig running. Material two is a regular tin based solder. Material three is a gallium alloy which is in liquid state at room temperature with a boiling point higher than 1350 °C. This alloy is commercially available under the name Coollaboratory Liquid Pro with application as thermal interface material for computer processors.

The position of the piston (Fig. 2H) as the clutch engages is measured by a contact DVRT (differential variable reluctance transducer) sensor (Fig. 3) mounted at the back of the clutch drum. The sensor pin is spring loaded and follows the piston as it moves. The maximum length of movement that can be measured by the sensor is 6 mm and it gives resolution down to single micrometers. The output is a voltage that is calibrated against a test curve and interpreted in the post processing of experimental data. The change in distance traveled by the piston during an engagement over a

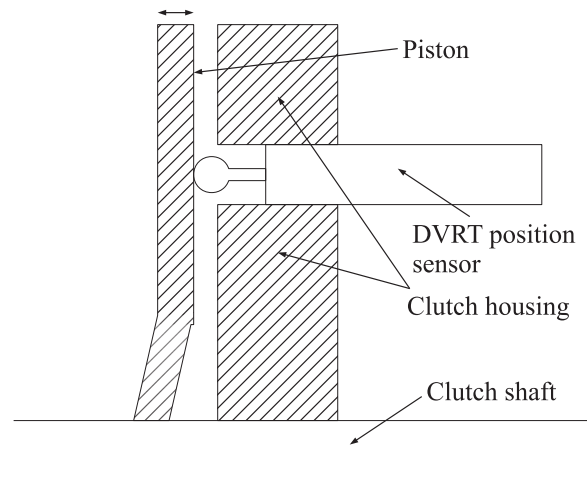


Fig. 3. Schematic of position sensor measurement setup.

test series will yield information about the thickness change of the clutch pack, thus yielding information about wear.

The hydraulic actuating pressure which controls the clutch engagement is continuously measured by a pressure sensor which is also mounted at the back of the clutch drum. The sensor measures relative pressure increase with a response time less than 1 ms. The pressure measurement is directly related to the axial force and clutch disc face pressure through the piston area.

The rotational speed of the system is measured by a mechanical counter built into the electric motor that accelerates the rig. For one revolution of the shaft, 4096 pulses are sent from the motor. A set time interval is specified and the number of pulses are counted within this interval, giving the rotational speed. In this investigation, the number of pulses were sampled at a rate of 100 Hz.

2.3. Data retrieval and system control

The test rig is controlled by a Compact Rio computer through a LabView interface running on a PC. The computer in turn controls several sub systems; electric motor controller, the hydraulic pump and valves, the pumps for the cooling and lubrication of the clutch.

The hydraulic pump and valve controlling clutch engagement is switched on and off through simple digital switches in the control program. In the current setup, the hydraulic pump yields a system pressure of 5 MPa. The servo solenoid valve controlling the actuating pressure is controlled through a feedback loop including a control channel. Any sensor reading can be used as the control channel, but in the present cases the actuating pressure reading governs the valve action. The pressure sensor reading is compared to the desired pressure and combined into a control voltage fed to the valve. The response time for the valve is less than 5 ms, allowing for precise control of the actuating pressure.

The test rig can run in two modes. One where everything is controlled manually and one which is a sequence based running mode. In the second mode, a test sequence can be specified and set to run a number of clutch engagements. This mode is ideal for running extended wear tests on a clutch pack. The manual control is mainly useful for testing sensors and test rig functionality.

The computer also handles the data retrieval, saving the data on an external hard drive in binary form. Data is only stored during the actual clutch engagement, which lasts for approximately 1 s. The system samples the data at a rate of 2000 Hz, enough to resolve all the phenomena present during the engagement.

Parallel to the control system, there is a security system including relays to switch off power if the temperature or actuating pressure exceeds a preset value. There are also relays for

Table 2
Sensor working range and resolution.

Quantity	Working range	Resolution	Manufacturer and model
Actuating pressure [MPa] ⇒ Axial force [N]	0–10 (0–2.67)×10 ⁴	0.05 128.5	Tecsis P3349
Piston displacement [mm] Torque arm load [N] ⇒ Torque [N m]	0–6 50–20,000 7.5–3000	0.0006 100 15	Microstrain DVRT Sensy 5960
Temperature [°C]	< 600	3 at 100 °C	Pentronic 8105000

Table 3
Friction disc geometrical properties.

	Type A	Type B
Groove pattern	Waffle	Waffle
Groove width	1 mm	1.4 mm
Groove depth	0.35 mm	0.25 mm
Contact patch size	6.2 mm × 6.2 mm	5.8 mm × 5.8 mm
Friction material thickness	0.50 mm	0.47 mm

lubrication and hydraulic oil levels. A final relay will switch off the power in 30 s if it has not received a pulse from the controller within that time. These systems will protect the rig from damage in case of software failure or excessive oil leakage.

The discrepancy between the 2000 Hz sample rate of the system and 100 Hz sample rate of the rotational speed results in a stair shape in the rotational speed curve. This is handled by processing the speed data using interpolation which yields a smooth curve, which is necessary in order to produce well defined friction versus sliding speed curves.

The coefficient of friction is calculated directly from the torque measurement and the measurement of engagement pressure through the equation

$$\mu = \frac{T}{n(A_p p - F_s)R_f} \quad (1)$$

Here n is the number of friction interfaces, A_p the area of the piston, p is the hydraulic actuating pressure, F_s is the force exerted by the return spring and R_f is the mean radius of the friction discs. The spring force is calculated via the piston position measurement. All of this is done for each measurement point which allows for matching between the friction measurement and the speed measurement to construct a plot over the friction versus speed behavior.

2.4. Test specimens and lubrication

The clutch discs tested are paper based friction discs and steel separator discs. The clutch friction material surface has an outer diameter of 148.5 mm and an inner diameter of 114.2 mm. These dimensions are the standard friction disc dimensions for the clutch axle used in the test rig.

Table 4
Varied parameter and its effect on engagement braking power.

	Actuating pressure [MPa]		
	0.8	1.3	1.8
Nominal surface pressure [MPa]	2.0	3.3	4.6
Maximum power [W]	1.2 × 10 ⁵	1.6 × 10 ⁵	2 × 10 ⁵
Mean power [W]	6.0 × 10 ⁴	9.4 × 10 ⁴	1.3 × 10 ⁵
Max specific power [W/m ²]	5.7 × 10 ⁶	7.9 × 10 ⁶	9.8 × 10 ⁶
Mean specific power [W/m ²]	2.9 × 10 ⁶	4.5 × 10 ⁶	6.3 × 10 ⁶

Two different types of friction discs have been used to evaluate the test rig performance. Material A is a paper type friction material designed to have a good balance of frictional characteristics and mechanical strength with a large amount of synthetic fibers. Material B is a paper type material used in many construction equipment drivetrains. Differences in the geometry of the friction discs are summarized in Table 3.

The lubricant used is Volvo Transmission Oil 97342 defined in Volvo Corporate Standard 1273,42 [14]. The ATF has a viscosity of 34 cSt at 40 °C and 5.5 cSt at 100 °C.

2.5. Test series

Initial tests have been performed to assess the ability of the test rig to measure clutch wear, temperature and engagement characteristics. The tests have been performed at one single energy level, 3.12 × 10⁴ J, corresponding to a rotational speed of 3000 rpm. In terms of specific energy this equals 1.51 × 10⁶ J/m². The parameter varied is the hydraulic actuating pressure which influences the surface pressure and power as shown in Table 4 based on the properties of friction material A.

Using these settings, 25,000 engagements were performed during 120 h. The clutch pack was removed every 5000 engagements for mechanical measurements using a micrometer screw gauge. The measurement was performed by squeezing the clutch pack between two steel plates loaded by a spring, yielding a force of 450 N, whereupon the clutch pack thickness was measured at four points. Based on these four measurements a mean clutch pack

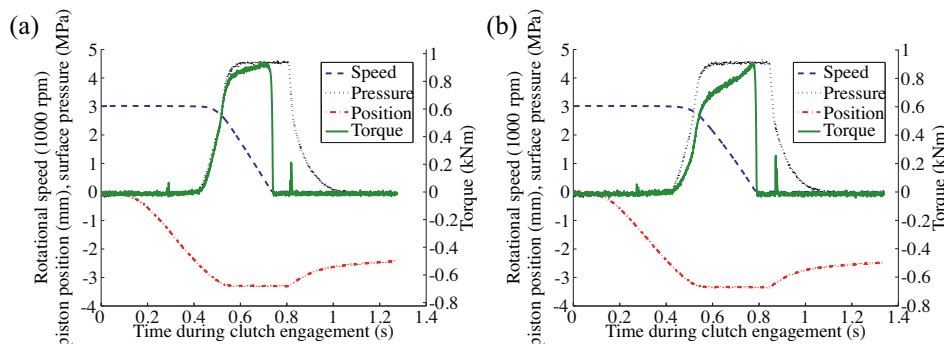


Fig. 4. Clutch engagement characteristics for the two friction materials: (a) material A and (b) material B.

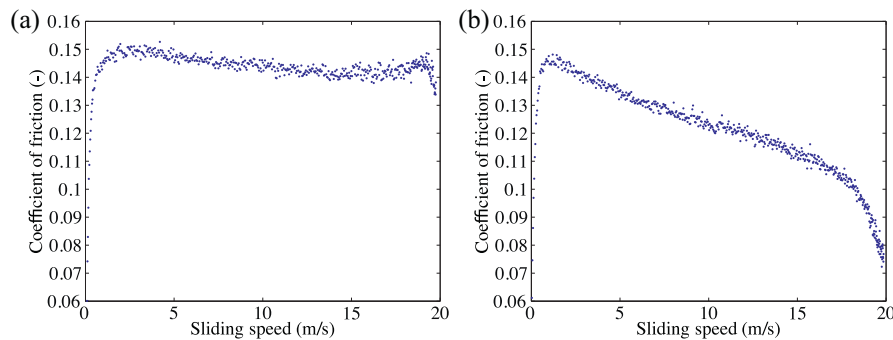


Fig. 5. Friction characteristics: (a) material A and (b) material B.

thickness and a standard deviation for the measurement variation was calculated.

Extra care was taken to reassemble the clutch pack with all discs oriented the same way as before disassembly. This was necessary due to tendencies of the position sensor to detect a temporary difference in piston stroke when the clutch pack orientation changed.

The heat exchanger controlling the oil temperature was set such that the steady state oil temperature in the tank was 45 °C. In this test series the only source of heat was friction induced heat in the clutch.

The test sequence was performed once using Material A for actuating pressures 0.8 and 1.3 MPa. At the pressure 1.8 MPa three repetitions of the experiment was performed using Material A and one test was performed using Material B.

A separate test was performed to decide which type of thermal interface material was to be used for the thermocouples. This was done at a much lower energy, 1.46×10^4 J with the actuating pressure 1.3 MPa (nominal surface pressure of 3.3 MPa). This energy corresponds to a rotational speed of 2050 rpm. The thermocouples were inserted into three different holes in the same separator disc in order to obtain a good comparison. This was done since it was necessary to determine which temperature measurement method was the most suitable prior to initiation of actual wear tests.

A third test was also performed to assess the wear behavior during the first 100 clutch engagement. In this case the actuating pressure used was 1.8 MPa and the engagement energy 3.12×10^4 J. The clutch pack was measured four times using the micrometer screw gauge; before first engagement, after first engagement, after 4 engagements and after 105 engagements.

3. Results and discussion

Two examples of how the output from one engagement can look is shown in Fig. 4, one with each friction material. These specific engagements are carried out using the operating conditions in the third column of Table 4. The initial movement of the piston is visible before the onset of torque transfer, being controlled by an initial filling pulse where the actuating pressure is increased from 0 to 0.05 MPa to bring the piston closer to the pressure plate. At the time of contact, the nominal surface pressure increases and so does the torque transfer while the piston is stationary, applying pressure on the clutch while the speed is decreasing almost linearly. As the speed reaches zero, the pressure is released after 0.1 s and the piston starts returning to the initial position.

There is a difference in the two materials performance during engagements. Material B has a slightly longer engagement time and is slower to reach a fully developed torque transfer than material A.

3.1. Friction characteristics

The torque curve is used to calculate the coefficient of friction during the engagement. Together with the speed curve it is possible to obtain a μ - v curve for the friction pair. The friction curves from the engagements in Fig. 4 is shown in Fig. 5.

Material A shows a steady friction coefficient from high to low speeds while material B shows a rising coefficient of friction as the velocity decreases. Both materials do, however, show a decrease in coefficient of friction as the velocity approaches zero. However, the low velocity (0–1 m/s) friction behavior should not be over interpreted in this case as it is difficult to determine the exact time when the sliding ceases using a dynamometer test rig.

At higher sliding speeds, the differences in frictional behavior of the two materials is clearly visible. Material A shows a high and steady friction throughout the engagement while material B shows an increasing coefficient of friction as the engagement proceeds and the sliding speed decreases. The highly negative μ - v slope of material B will lead to rougher gear shifts than the stable coefficient of friction of material A as the torque transfer will increase throughout the engagement although the engagement pressure is constant. The reason for the negative slope of material B is likely due to a stiffer and less porous structure, allowing for a mixed lubrication to a larger extent than for the more porous structure of material A.

In Fig. 6, a comparison between the friction coefficients at the beginning and at the end of the test series is plotted for material A. The plot suggests that the friction curve is satisfactory also towards the end of the test series. It also implies that the torque transfer properties of the clutch does not change significantly during the test duration.

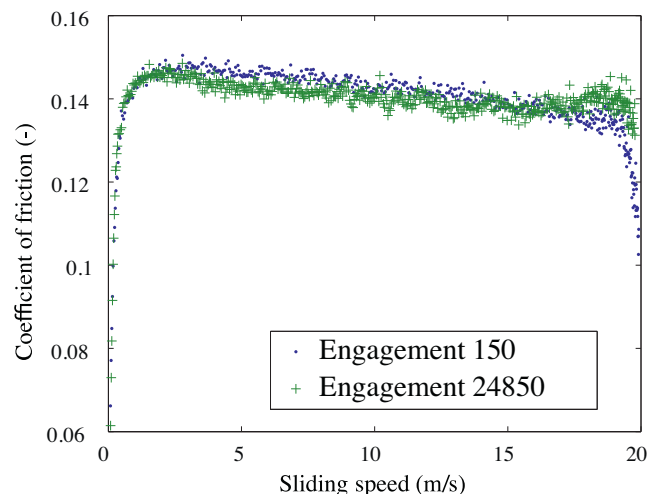


Fig. 6. Material A, friction characteristics over test series. Surface pressure: 4.6 MPa.

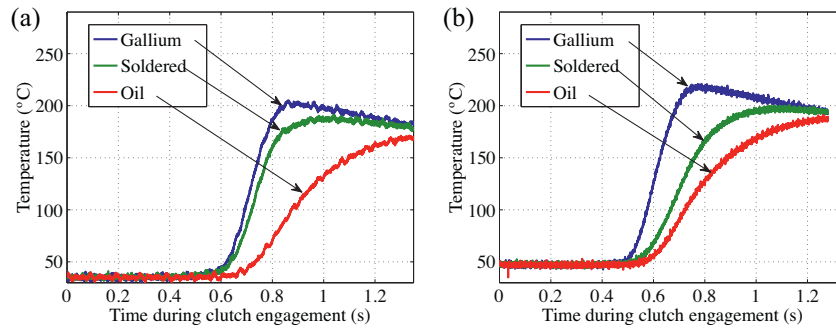


Fig. 7. Influence of using different thermal interface material: (a) engagement number 10 and (b) engagement number 1010.

3.2. Clutch temperature

The tests using different thermal interface materials for the thermocouples introduced in Section 2.2 yielded the temperature curves in Fig. 7. It is easy to argue that there are large differences in the performance of the different materials. Having only the oil as a conductor will yield a slow response while a soldered thermocouple and a thermocouple with the gallium alloy as an interface material will yield much shorter response times. However, the soldering medium will melt and solidify multiple times during a test series, causing a deterioration of the thermal contact between separator disc and thermocouple. The gallium alloy, however, provides a stable interface material that lasts during a long test series.

The temperature measured in the separator discs for the engagement in Fig. 4(a) is shown in Fig. 8. The curve reaching the highest values is the curve of the center separator disc. This is due to the fact that this disc has two rubbing interfaces, meaning that the center disc receives the heat from two sources while the two other separator discs only has one heat source. The disc with the higher cooling rate is the outer disc in direct contact with the steel washer which serves as a heat sink.

3.3. Clutch wear

The wear of the clutch can be directly correlated to the change in thickness of the clutch pack which can be measured through the distance traveled by the piston during engagement. The curves in Fig. 9 show the measured increase in distance traveled by the piston during the engagement over a test series of about 25,000 engagements with each point of the plot being a measurement for one engagement. The error bars represent the standard deviation of the mean clutch pack thickness measured using the micrometer screw

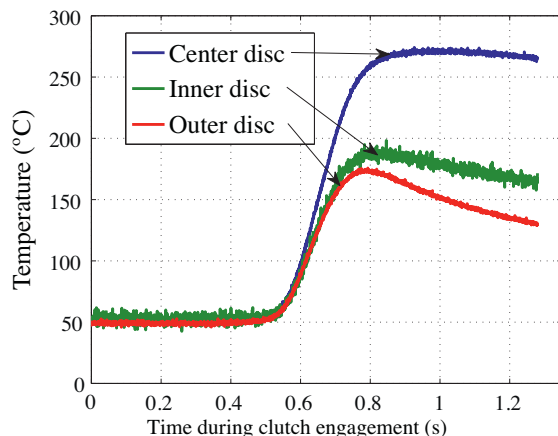


Fig. 8. Separator disc temperatures.

gauge with the mean thickness change as the mean value. Simultaneous plotting of these allows for determination of the accuracy of the test rig measurements.

The thickness change of the clutch pack measured using the micrometer screw gauge is represented by the error bars in the figures for comparison between the two measurement methods.

The location of the zero wear point is determined by linear curve fitting to the first 5000 engagements while the micrometer measurement result is synchronized with a mean value of the engagements between 4900 and 5000. This is done due to the initial running in effects that are visible in the micrometer measurements. In this initial phase, the thickness of the clutch pack decreases significantly. Most of the thickness decrease does occur during the first engagement. After the first few engagements, the clutch thickness decrease stabilizes and follows the test rig measurements seen in Fig. 9.

The plots in Fig. 9 are ordered by increasing engagement pressure, with (a) being the lowest pressure, (b) being the intermediate pressure and (c), (d), and (e) being the high pressure. The plot in (f) also represents a high pressure test series, but with material B while (a)–(e) is material A.

Differences between the materials and engagement pressures can clearly be discerned. Wear of the friction material is detected by the piston position sensor and the measurements agree well with the results from the micrometer screw gauge. The position sensor also makes it possible to analyze changes in wear behavior during the course of the experiment such as can be seen in (c)–(e) in Fig. 9 in greater detail.

There is a variation in the position sensor measurements that spans about 40 μm . If zoomed in upon, the variation is shown to have a periodic nature (Fig. 10), indicating that this is due to something akin to rotational movement of the piston. This means that taking a mean value over a period would yield a representative value for the wear.

There is also an anomaly at the points where the clutch pack was removed to be measured. The result is a higher thickness reading which decays during the first engagements of the continued test. The same thing can also be seen at a few other points, where the test rig has been allowed to rest for some hours. The decay of the thickness reading difference coincides perfectly with the increase of temperature at the position sensor, meaning that it is possible to correct for this behavior with the help of temperature data near the position sensor.

The fact that most of the initial thickness decrease of the clutch pack occurs during the first engagement is evident from Fig. 10 where the results from the test covering the first 105 engagements is shown. This can be seen as the settling of the material into a new stable structure through plastic deformation due to the pressure applied during this initial engagement. As the test is continued, this structure does not seem to change significantly. The amount of clutch pack thickness decrease during the first engagement

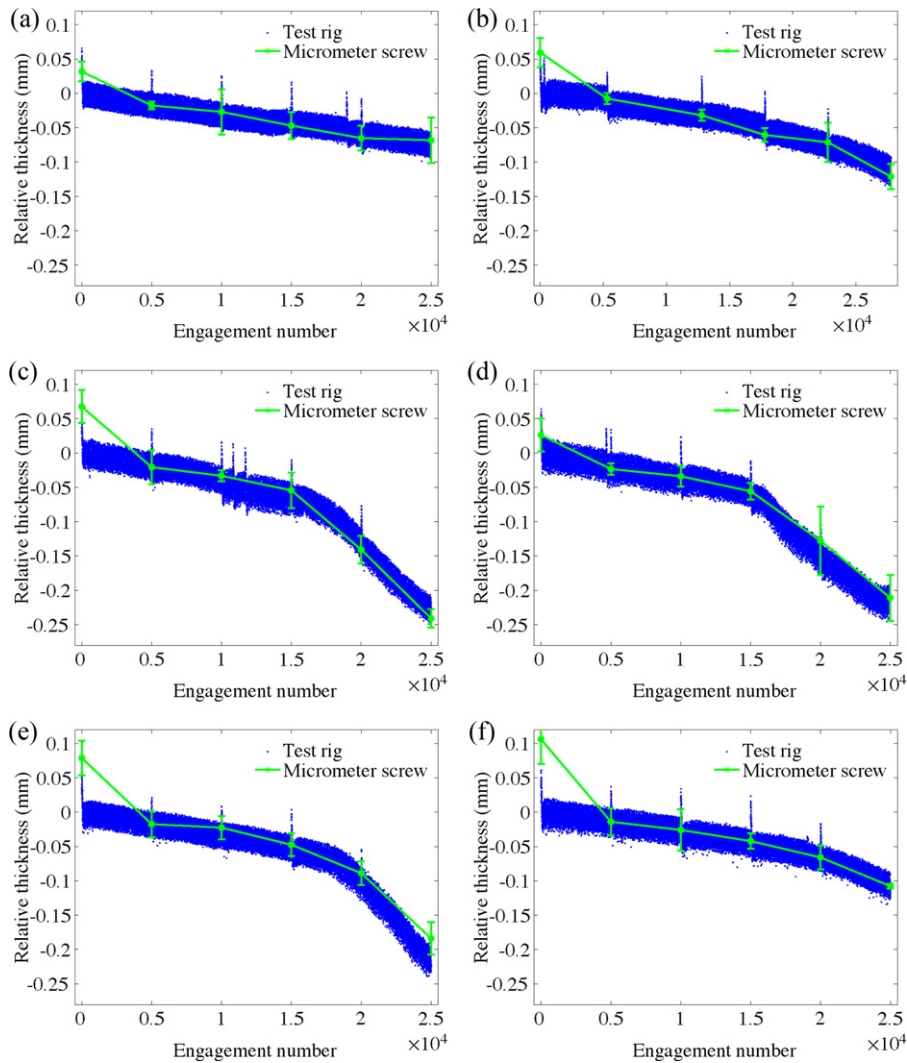


Fig. 9. Wear behavior during 6 different test series: (a) material A, surface pressure: 2.0 MPa, (b) material A, surface pressure: 3.3 MPa, (c) material A, surface pressure: 4.6 MPa, Test 1, (d) material A, surface pressure: 4.6 MPa, Test 2, (e) material A, surface pressure: 4.6 MPa, Test 3, and (f) material A, surface pressure: 4.6 MPa.

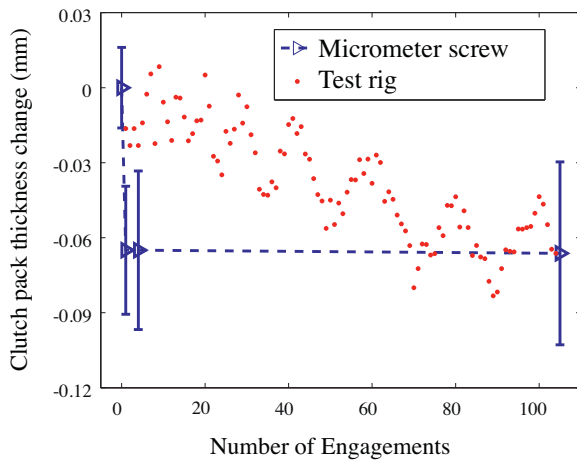


Fig. 10. Initial wear behavior: material A, surface pressure: 4.6 MPa.

corresponds well with the difference between the first micrometer screw gauge results and the fitted zero wear point in Fig. 9(c)–(e).

The measurements obtained from the test rig in Fig. 10 does not capture this initial change since the distance traveled by the

piston to obtain full compression is the same throughout this initial phase. The slow change in measured clutch pack thickness is the thermal effect and levels out as the test rig reaches an equilibrium temperature after about 100 engagements.

Fig. 11 shows the appearance of friction material A before and after subjection to a wear test. The unworn material has more visible fibers and pores than the worn one. If zoomed in upon, the surface of the worn sample has features indicating that it is a lot flatter, which could either be from deposition of glaze or truncation of all the rough peaks of the friction material. However, clear traces indicating that wear has occurred does not show on the surface in the SEM.

The reason for the change in wear rate seen in Fig. 9 c,d and e is unclear. However, the sudden nature of the wear rate change indicates that there could be some kind of fatigue mechanism lying behind this behavior. It could be a thermal fatigue mechanism as proposed by Okabe et al. [15], or a mechanical fatigue mechanism akin to the one identified by Chiba et al. [16]. The phenomenon has been observed only at the highest engagement power. However, it cannot be ruled out that the same phenomenon exists at lower powers and energies. Therefore the mechanisms behind the wear rate change will be investigated further using the test rig and other methods.

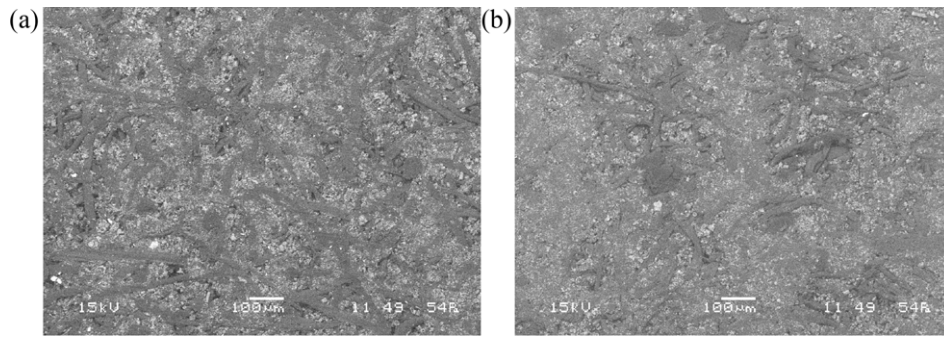


Fig. 11. SEM images of friction material A: (a) unworn material and (b) worn in the test sequence shown in Fig. 9(c)–(e).

4. Conclusions

The wet clutch wear rig described here can be used to measure several clutch characteristics. The position of the piston gives a very good indication as to how the wear of the clutch pack is proceeding and can point out critical occurrences during clutch operation. In addition to the wear data, temperature data for the separator discs in proximity to the friction interfaces is measured. This allows for investigations on how wear and friction material properties depend on surface temperature.

Engagement time, torque transfer and friction properties for the clutch are secondary measured parameters of interest. Information about how these properties vary with regards to amount of energy that is being dissipated during engagement and the power dissipated will be the result from experiments using the test rig.

The bend in the wear curve for material A indicates that after a certain number of engagements at high energies and powers, the wear rate increases which could lead to premature failure of the clutch. This phenomenon is subject for future investigations using the test rig.

Acknowledgements

We would like to thank Mr. Jan Granström for his aid in developing the control system for the test rig. We would also like to thank the Swedish energy agency through the Swedish research program FFI for the financial support for this work.

References

- [1] A. Anderson, Friction and wear of paper type wet friction materials, SAE Paper (720521).
- [2] G. Huron, Numerical simulations of SAE #2 machine tests, SAE Technical papers (1999-01-3617).
- [3] S. Sanda, Frictional characteristics of a wet clutch composed of paper-based facings during the running-in process, Japanese Journal of Tribology 39 (12) (1994) 1495–1504.
- [4] M. Holgersson, Apparatus for measurement of engagement characteristics of a wet clutch, Wear 213 (1997) 140–147, doi:10.1016/S0043-1648(97)00202-0.
- [5] R. Mäki, B. Ganemi, R. Olsson, B. Lundström, Limited slip wet clutch transmission fluid for AWD differentials; part 1: system requirements and evaluation methods, SAE Technical papers (2003-01-1980).
- [6] V. Ivanović, Z. Herold, J. Deur, M. Hancock, F. Assadian, Experimental setups for active limited slip differential dynamics research, SAE Technical Papers (2008-01-0302).
- [7] P. Marklund, R. Larsson, Wet clutch friction characteristics obtained from simplified pin on disc test, Tribology International 41 (9–10) (2008) 824–830.
- [8] W. Ost, P. Baets, J. Degrieck, The tribological behaviour of paper friction plates for wet clutch application investigated on SAE #2 and pin-on-disc test rigs, Wear 249 (2001) 361–371.
- [9] K. Berglund, P. Marklund, R. Larsson, Lubricant ageing effects on the friction characteristics of wet clutches, Proceedings of the Institution of Mechanical Engineers, Part J: Journal of Engineering Tribology 224 (7) (2010) 639–647, doi:10.1243/13506501JET734.
- [10] T. Newcomb, M. Sparrow, B. Ciupak, Glaze analysis of friction plates, SAE Technical Papers (2006-01-3244).
- [11] M. Ingram, H. Spikes, J. Noles, R. Watts, Contact properties of a wet clutch friction material, Tribology International 43 (4) (2010) 815–821, doi:10.1016/j.triboint.2009.11.008.
- [12] Y. Kimura, C. Otani, Contact and wear of paper-based friction material for oil-immersed clutches—wear model for composite materials, Tribology International 38 (2005) 943–950, doi:10.1016/j.triboint.2005.07.033.
- [13] T. Saito, T. Kotegawa, Y. Matsuura, S. Tanaka, K. Ohtsuki, Study of durability prediction with focus on wear properties for multiple plate clutches, SAE Technical Paper Series (2007-01-0240).
- [14] Volvo corporate standard, transmission oil 97342, <http://www.tech.volvo.com/std/docs/1273.42> (April 29, 2011).
- [15] K. Okabe, A. Fujimoto, T. Harasawa, Proposal of field life design method of wet multiple plate clutches of automatic transmission on forklift-trucks, SAE Technical Papers (2009-01-2934).
- [16] N. Chiba, M. Kano, M. Inoue, Mechanism of compression fatigue of wet friction materials, JSAE Review 22 (2) (2001) 169–174.